Science of the Total Environment 625 (2018) 246–251

Contents lists available at ScienceDirect

Science of the Total Environment

journal homepage: www.elsevier.com/locate/scitotenv

Light absorption properties of brown carbon over the southeastern Tibetan Plateau

Chong-Shu Zhu [a,*], Jun-Ji Cao [a], Ru-Jin Huang [a], Zhen-Xing Shen [b], Qi-Yuan Wang [a], Ning-Ning Zhang [a]

[a] Key Laboratory of Aerosol Chemistry & Physics, SKLLQG, Institute of Earth Environment, Chinese Academy of Sciences, Xi'an 710061, China
[b] Department of Environmental Science and Engineering, Xi'an Jiaotong University, Xi'an 710049, China

HIGHLIGHTS

- The light-absorbing properties of WS-BrC and MeS-BrC were investigated in the southeastern Tibetan Plateau.
- Mass absorption cross section of BrC in the southeastern Tibetan Plateau has a strong seasonal variability.
- BrC was the dominant absorption material in extracts.

GRAPHICAL ABSTRACT

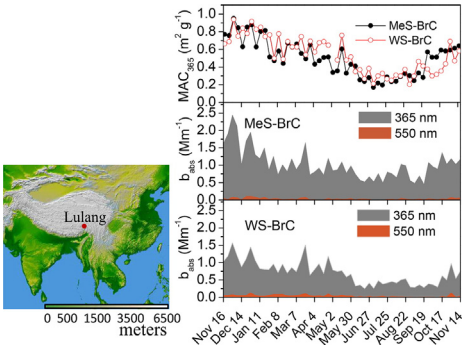

ARTICLE INFO

Article history:
Received 5 November 2017
Received in revised form 12 December 2017
Accepted 17 December 2017
Available online 28 December 2017

Editor: Jianmin Chen

Keywords:
Brown carbon
Light absorption coefficient
Mass absorption cross section
Tibetan Plateau

ABSTRACT

We present a study of the light-absorbing properties of water-soluble brown carbon (WS-BrC) and methanol-soluble brown carbon (MeS-BrC) at a remote site (Lulang, 3326 m above sea level) in the southeastern Tibetan Plateau during the period 2015–2016. The light absorption coefficients at 365 nm (b_{abs365}) of WS-BrC and MeS-BrC were the highest during winter and the lowest during monsoon season. MeS-BrC absorbs about 1.5 times higher at 365 nm compared to WS-BrC. The absorption at 550 nm appears lower compared to that of 365 nm for WS-BrC and MeS-BrC, respectively. Higher average value of the absorption Ångström exponent (AAE, 365–550 nm) was obtained for MeS-BrC (8.2) than that for WS-BrC (6.9). The values of the mass absorption cross section at 365 nm (MAC_{365}) indicated that BrC in winter absorbs UV–visible light more efficiently than in monsoon. The results confirm the importance of BrC in contributing to light-absorbing aerosols in this region. The understanding of the light absorption properties of BrC is of great importance, especially in modeling studies for the climate effects and transport of BrC in the Tibetan Plateau.

1. Introduction

Brown carbon (BrC) is a certain type of organic carbon (OC), which absorbs radiation efficiently at the blue and ultraviolet (UV) wavelength of the solar spectrum (Pöschl, 2003; Andreae and Gelencsér, 2006; Moosmüller et al., 2011). BrC may contribute substantially the total aerosol absorption at specific wavelengths, thereby affecting the accuracy of climate model results and satellite data retrieval. The light absorption of BrC produced from different types of biofuels burning under varied combustion conditions have been investigated (Ramanathan et al., 2007a, 2007b; Alexander et al., 2008; Andreae and Gelencsér, 2006). The previous studies showed that BrC (including

* Corresponding author at: Institute of Earth Environment, Chinese Academy of Sciences, No. 97 Yan xiang Road, Yan-ta Zone, Xi'an 710061, Shaanxi, China.
E-mail address: chongshu@ieecas.cn (C.-S. Zhu).

https://doi.org/10.1016/j.scitotenv.2017.12.183
0048-9697/

primary and secondary BrC) is typically emitted during biomass burning, coal combustion, and the formation of secondary organic aerosol (SOA) (e.g., Hecobian et al., 2010; Lack and Langridge, 2013; Zhang et al., 2013; Laskin et al., 2015).

The light absorption of BrC is estimated by either measuring the absorption of organics extracted in water, acetone, methanol, or by calculating the difference between total absorption and that of black carbon (BC) (Chen and Bond, 2010; Laskin et al., 2015). At present, the transformations mechanisms and rates of BrC are not well characterized, and little is known about the relationship among the chemical components and its light absorption properties.

The Tibetan Plateau (TP), called as "the third pole" with the extremely high altitude, is an important and vulnerable region for the changes of global climate and regional environment. The TP glaciers determine the albedo of the area with snow cover, and provide the water of some Asian rivers. These rivers are important water resources for billions of local habitants in surrounding areas (Yao et al., 2012). The series effects of carbonaceous aerosol (e.g., BC and BrC) are attracting attention recently, because of their considerable role in the melting of glaciers and the albedo effects in the TP (e.g., Cao et al., 2009; Xu et al., 2009, 2012; Wang et al., 2012; Cong et al., 2013; Zhu et al., 2017). Long-range transport from upwind regions to the plateau is the major source of pollutants (Cao et al., 2010; Zhu et al., 2017). The abundant BrC in Indo-Gangetic Plain could enter the TP from the south side of the Himalayas, and may exert profound impacts on the climate and regional environment (Srinivas and Sarin, 2013, 2014; Zhao et al., 2013; Srinivas et al., 2016). The investigations for the chemical composition and absorption properties of BrC in the TP are needed. Until now, very few studies focused on the light-absorbing properties of water-soluble brown carbon (WS-BrC) and methanol-soluble brown carbon (MeS-BrC) were conducted in the TP.

In this work, an attempt has been made to investigate the light properties of WS-BrC and MeS-BrC in the southeastern TP. The relationships between BrC light absorption and carbonaceous fractions are also investigated during the sampling period.

2. Materials and methods

2.1. Sampling

The field aerosol sampling campaign was conducted at Lulang (94.73°E, 29.76°N, 3326 m a.s.l.) in southeastern region of the TP (Fig. 1). The map presents the seasonal aerosol optical depth, retrieved from satellite (Terra/Modis) observations during the sampling period (http://www.nasa.gov). The detailed description about the sampling site has been reported elsewhere (Cao et al., 2010; Zhao et al., 2013).

Total suspended particulate (TSP) samples (47 mm Whatman quartz–fiber filters, with filter changing at 1000 local standard time) were collected on a weekly basis at 17 L/min with a custom-built sampler from November 2015 to November 2016. The field blank samples in southeastern TP were also collected during the sampling period. These quartz–fiber filters were pre-heated at 900 °C for 3 h to remove the residual carbon. The samples were stored in a refrigerator at about −20 °C to prevent the volatile components evaporation after sampling.

2.2. Measurement of carbonaceous fractions

All the filters (including field blank filters) were analyzed for carbon fractions by using a DRI Model 2001 Thermal/Optical Carbon Analyzer (Atmoslytic Inc., Calabasas, CA, USA). Carbon fractions were analyzed following the IMPROVE-A (Interagency Monitoring of Protected Visual Environments) thermal/optical reflectance (TOR) protocol (Chow et al., 2007). The concentrations of organic carbon (OC) and elemental carbon (EC) were obtained. The detailed procedures for quality assurance and quality control (QA/QC) have been reported elsewhere (Cao et al., 2003; Chow et al., 2011).

A part of the TSP sample was cut into pieces, and then extracted with Milli–Q water (30 mL) three times (60 min, 20 min for each cycle) under sonication, and filtered by using the Polytetrafluoroethylene (PTFE) filters. The combined water extracts were analyzed for water-soluble organic carbon (WSOC), water–soluble inorganic carbon (WSIC) and water-soluble total nitrogen (WSTN) by using the Shimadzu TOC–L CPH Total Carbon/Nitrogen Analyzer (Wang et al., 2010). Major water-soluble inorganic nitrogen (WSIN) species in atmospheric aerosols are NO_3^- and NH_4^+, thus the difference between WSTN and WSIN is defined as water-soluble organic nitrogen (WSON) (Wang et al., 2013). Temporal variability of WSOC and water-soluble organic nitrogen (WSON) concentrations for TSP during the sampling period was obtained.

2.3. Measurements of the light-absorbing properties of BrC

BrC was extracted from the filter subsamples by 1 h sonication in ultrapure Milli–Q water (>18.2 MΩ) or from the filter subsamples by 1 h sonication in methanol (J. T. Baker, HPLC Grade). The water and methanol extracts were then filtered to remove these insoluble material using 0.22 μm PES (polyether sulphone) and 0.45 μm PTFE pore syringe filter, respectively. Absorption spectra of the extracts (water or methanol) were measured using a Liquid Waveguide Capillary Cell (LWCC–3100, World Precision Instrument, Sarasota, FL, USA, 0.94 m in length) equipped with a UV–Vis spectrophotometer (300–700 nm) (Hecobian et al., 2010; Laskin et al., 2015; Kirillova et al., 2016). The light

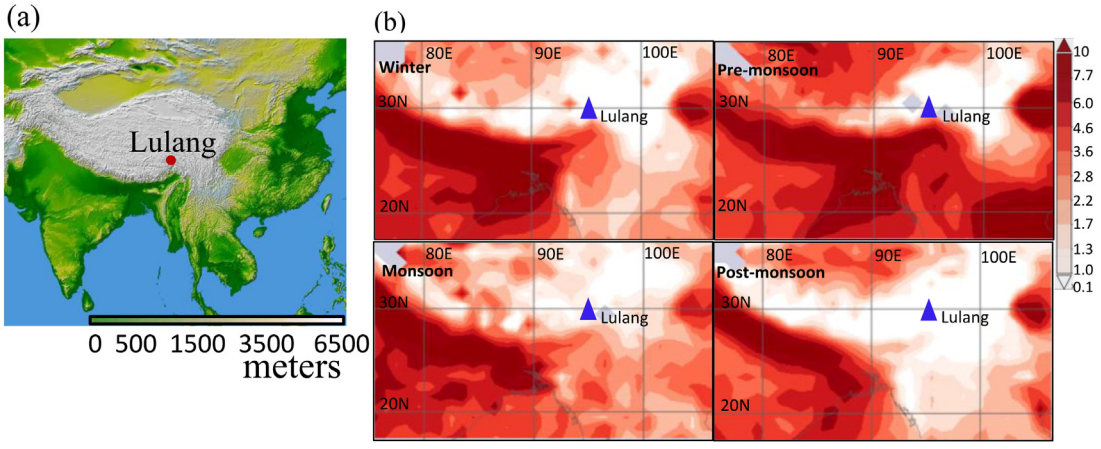

Fig. 1. Geographic location of the sampling site, Lulang (a). Time averaged maps of the seasonal AOD were produced with the Giovanni online data system, developed and maintained by the NASA GES DISC (b).

absorption data were then converted to the BrC absorption coefficient following Eq. (1)

$$b_{abs\lambda} = (A_\lambda - A_{700}) \frac{V_l}{V_a \times l} \times \ln(10) \quad (1)$$

where $b_{abs\lambda}$ (Mm^{-1}) represents the absorption coefficient of filter extracts at wavelength of λ. A_λ (arbitrary unit) is the light absorbance recorded. V_l (in mL) corresponds to the volume of solvent (water or methanol) used to extract the filter sample, and V_a (in m^3) is the volume of the air sampled through the filter punch. The optical length (l) of LWCC used here is 0.94 m and ln(10) converts the log base-10 (recorded by UV–Vis spectrophotometer) to nature log to be consistent with the typical atmospheric measurement results. To account for baseline shift that may occur during analysis, absorption at all wavelengths below 700 nm are referenced to that of 700 nm (no absorption for ambient aerosol extracts). The average absorption coefficient between 360 and 370 nm (b_{abs365}) is used to represent BrC absorption in order to avoid interferences from non-organic compounds (e.g., nitrate) and to maintain consistence with previous reported results.

The light absorption wavelength (λ) dependences for WS-BrC and MeS-BrC were obtained using the absorption Ångström exponent (AAE) (Moosmüller et al., 2011). In this study, the two-wavelength AAE is defined as:

$$AAE = -\frac{\ln\left(\frac{p_{365nm}}{p_{550nm}}\right)}{\ln\left(\frac{365}{550}\right)} = -\frac{\ln(p_{365nm}) - \ln(p_{550nm})}{\ln(365) - \ln(550)} \quad (2)$$

where p_{365nm} and p_{550nm} are absorption coefficients at the wavelengths of 365 nm and 550 nm, respectively.

The mass absorption cross section (MAC) for water and methanol extracts was computed at 365 nm using the following equation:

$$MAC_{365} = \frac{(A_{365} - A_{700}) \times \ln(10)}{C_{(WS)OC} \times l} \quad (3)$$

where $C_{(WS)OC}$ is the concentration of WSOC in water solution or OC in the methanol solution. We assumed that methanol extracts almost all OC from the filter (Chen and Bond, 2010).

3. Results and discussion

3.1. Seasonal and weekly variations of TC, OC, WSOC, and WSON concentrations

Fig. 2 showed the seasonal variations of total carbon (TC), OC, WSOC, and WSON levels at the Lulang site. The weekly average TC and OC concentrations showed large variability during the study period. TC varied over 2.8 folds from 1.6 to 4.6 μg m^{-3}, and OC varies over 3.2 folds from 1.1 to 3.5 μg m^{-3}. The TC and OC exhibited similar seasonal cycle, with the highest concentration observed during the monsoon (3.3 ± 0.7 μg m^{-3} and 2.5 ± 0.6 μg m^{-3} for TC and OC, respectively) and the lowest value during the pre-monsoon (2.6 ± 0.7 μg m^{-3} and 1.9 ± 0.6 μg m^{-3} for TC and OC, respectively). The TC and OC concentrations in the monsoon period were higher by about a factor of 1.3 compared with their mean values during the pre-monsoon.

The weekly concentrations of WSOC ranged from 0.7 μg m^{-3} to 2.8 μg m^{-3}, with an average value of 1.3 μg m^{-3}. The seasonal variations of WSOC were relatively constant throughout the year at Lulang with the levels for winter (1.41 ± 0.36 μg m^{-3}), pre-monsoon (1.39 ± 0.48 μg m^{-3}), post-monsoon (1.24 ± 0.25 μg m^{-3}), and monsoon (1.22 ± 0.34 μg m^{-3}), respectively.

As shown in Fig. 2, major peaks in the TC concentrations always coincided with high loadings of OC, and WSOC. This implies that the same physical processes, including those during both production and transport, caused these species' concentrations to covary. The seasonality of TC and OC we observed at Lulang is different from the variations observed at other sites in Nepal and India; that is, lower loadings during the monsoon season and higher concentrations in the winter and pre-monsoon periods (Ganguly et al., 2006; Marinoni et al., 2010; Mouli et al., 2006). High concentrations of TC and OC at Lulang may be attributed to the bioaerosol and vehicle emissions due to the local extensive forests and vehicular traffic (peak travel season) during monsoon (Shrestha et al., 2000). The aerosol transport pathways driven by the southwestern monsoon often pass over densely populated areas of the Indo-Gangetic Plain, so the variations of carbonaceous species at Lulang can be partially linked to the air flow (Marinoni et al., 2010). Comparable levels of WSON were found in four seasons in the range of 0.06 μg m^{-3} (winter and post-monsoon) to 0.08 μg m^{-3} (pre-monsoon and monsoon) (Table 1).

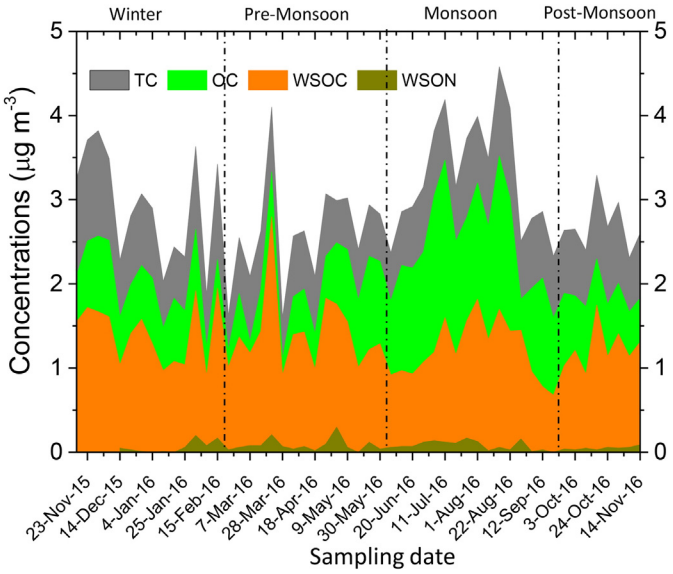

Fig. 2. Temporal variability of total carbon (TC), organic carbon (OC), water-soluble organic carbon (WSOC), and water-soluble organic nitrogen (WSON) for TSP during the sampling period.

3.2. Light absorption by BrC in water and methanol extracts

3.2.1. Brown carbon light absorption coefficient

Fig. 3 showed the time trend of the brown carbon absorption coefficients for WS-BrC and MeS-BrC at Lulang from November 2015 to November 2016. The light absorption coefficient of WS-BrC at 365 nm (b_{abs365}) correlated with the b_{abs365} of MeS-BrC. The weekly average values of b_{abs365} showed large variability during the study period. B_{abs365} varied over 6 folds from 0.25 to 1.57 Mm^{-1} for WS-BrC, and over 5 folds from 0.45 to 2.45 Mm^{-1} for MeS-BrC.

The mean WS-BrC b_{abs365} during winter, pre-monsoon, monsoon and post-monsoon seasons were 1.04 ± 0.25 Mm^{-1}, 0.85 ± 0.25 Mm^{-1}, 0.38 ± 0.09 Mm^{-1}, and 0.55 ± 0.23 Mm^{-1}, respectively. Compared to WS-BrC b_{abs365}, higher MeS-BrC b_{abs365} were obtained during winter, pre-monsoon, monsoon, and post-monsoon with the values of 1.47 ± 0.51 Mm^{-1}, 0.97 ± 0.24 Mm^{-1}, 0.67 ± 0.17 Mm^{-1}, and 1.09 ± 0.15 Mm^{-1}, respectively. The highest values of b_{abs365} were observed during the winter season for both of WS-BrC and MeS-BrC. The similar trends were observed for WS-BrC and MeS-BrC b_{abs550} with lower values compared to b_{abs365}.

The light absorption by MeS-BrC was on average 1.5 times higher at 365 nm than that by WS-BrC (Fig. 3 and Table 1). Assuming that OC is almost fully extracted by methanol (92% of primary OC) (Chen and Bond, 2010). The observed trend is in agreement with other studies, since methanol extracts a greater range of compounds than water

Table 1
Seasonal averages of the TC, OC, WSOC, and WSON concentrations, and the brown carbon absorption characteristics for the aerosols collected at Lulang. TSP samples were collected on a weekly basis from November 2015 to November 2016.

	Winter (n = 14)	Premonsoon (n = 15)	Monsoon (n = 16)	Postmonsoon (n = 8)
TC (μg m^{-3})	2.9 ± 0.6	2.6 ± 0.7	3.3 ± 0.7	2.7 ± 0.3
OC (μg m^{-3})	2.1 ± 0.4	1.9 ± 0.6	2.5 ± 0.6	1.9 ± 0.2
WSOC (μg m^{-3})	1.41 ± 0.36	1.39 ± 0.48	1.22 ± 0.34	1.24 ± 0.25
WSON (μg m^{-3})	0.06 ± 0.07	0.08 ± 0.08	0.08 ± 0.06	0.06 ± 0.02
b_{abs365} water (Mm^{-1})[a]	1.04 ± 0.25	0.85 ± 0.25	0.38 ± 0.09	0.55 ± 0.23
b_{abs365} methanol (Mm^{-1})	1.47 ± 0.51	0.97 ± 0.24	0.67 ± 0.17	1.09 ± 0.15
b_{abs550} water (Mm^{-1})	0.07 ± 0.02	0.06 ± 0.02	0.02 ± 0.01	0.03 ± 0.04
b_{abs550} methanol (Mm^{-1})	0.06 ± 0.03	0.03 ± 0.02	0.02 ± 0.02	0.04 ± 0.02
MAC_{365} water (m^2 g^{-1})[b]	0.75 ± 0.13	0.62 ± 0.09	0.32 ± 0.07	0.44 ± 0.14
MAC_{365} methanol (m^2 g^{-1})	0.71 ± 0.16	0.51 ± 0.12	0.27 ± 0.06	0.58 ± 0.05
AAE (365–550 nm) water[c]	6.7 ± 0.8	6.6 ± 0.6	7.2 ± 0.9	7.7 ± 1.3
AAE (365–550 nm) methanol	8.2 ± 1.4	8.4 ± 0.9	8.1 ± 0.9	8.0 ± 1.0

[a] b_{abs}: absorption coefficient.
[b] MAC: mass absorption cross section.
[c] AAE: absorption Ångström exponent.

(Chen and Bond, 2010; Liu et al., 2013; Zhang et al., 2013). The similar trends obtained for water and methanol extracts indicates that the higher b_{abs} recorded at short wavelengths for the methanol extracts with respect to water are mainly due to the fact that more organic matter is extracted in methanol than in water. In particular, the similar capacity of MeS-BrC and WS-BrC to absorb light at longer wavelength (550 nm) indicates that the organic compounds bearing chromophores capable to absorb light at long wavelengths can be extracted in both methanol and water. The ratio between WS-BrC b_{abs365} and MeS-BrC b_{abs365} reflects broadly the ratio of WSOC/OC in winter, pre-monsoon, and monsoon, which indicated both WSOC and water-insoluble OC contributes approximately equally to light absorption at short wavelengths.

Finally, it should be noted that the correction factors deriving the corresponding absorption coefficients from solutions for WSOC (OC) can be >1 (Sun et al., 2007). The BrC light absorption in aerosol is higher than the light absorption in the extracts of a factor of 2 for water extracts and a factor of 1.8 for methanol extracts at urban and rural sites in Georgia (Liu et al., 2013).

Fig. 4 showed scatter plots of WS-BrC b_{abs365} versus WSOC, and MeS-BrC b_{abs365} versus OC, respectively. Strong correlations (R values from 0.87 to 0.90 for WS-BrC, and from 0.85 to 0.92 for MeS-BrC) were observed in winter, pre-monsoon, and post-monsoon. The results

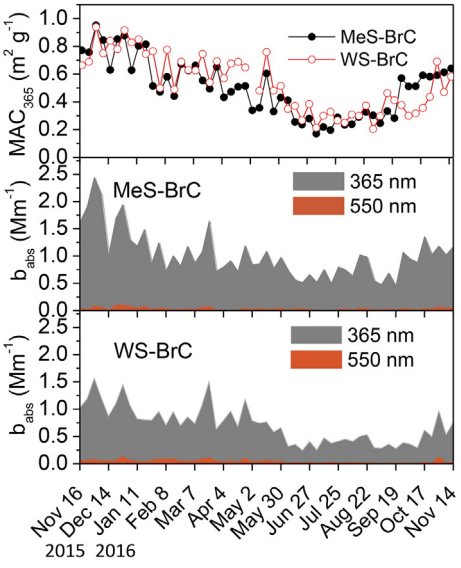

Fig. 3. Temporal variability of the mass absorption cross section at 365 nm (MAC_{365}), and light absorption coefficients at 365 nm (b_{abs365}) and 550 nm (b_{abs550}) for WS-BrC and MeS-BrC, respectively. No correction factor was applied.

indicated that BrC was the dominant absorption material in extracts and having similar sources to WSOC and OC, as reported in previous studies (Hecobian et al., 2010; Zhang et al., 2011; Shen et al., 2014). The lowest correlations were observed in monsoon with R values of 0.69 and 0.64 for WS-BrC and MeS-BrC, respectively. Large light absorbing secondary organic aerosols can be formed from photochemical processes in monsoon due to the local extensive forests and vehicular traffic emission (peak travel season). The results implied more sophisticated sources of BrC in summer than other seasons. The complexity of BrC and dynamic changes in its physicochemical properties make it especially challenging to investigate the relationship between its composition and absorption properties.

The linear relationship between the WS-BrC b_{abs365} and WSOC concentrations for water extracts are comparable with the previous studies in the Indo-Gangetic Plain (slope range: 0.7–1.13, R^2 range: 0.34–0.77) (Srinivas and Sarin, 2014; Srinivas et al., 2016). The previous study in southeastern United State also reported the lowest coefficient between b_{abs} and WSOC in summer (Hecobian et al., 2010).

3.2.2. Mass absorption cross section of BrC

The MAC results of the MeS-BrC and WS-BrC were given in Fig. 3. The mass absorption cross section values measured at 365 nm (MAC_{365}) in the water extracts for four seasons were 0.75 ± 0.13 m^2 g^{-1} (winter), 0.62 ± 0.09 m^2 g^{-1} (pre-monsoon), 0.32 ± 0.07 m^2 g^{-1} (monsoon), and 0.44 ± 0.14 m^2 g^{-1} (post-monsoon), respectively. In methanol extracts, MAC_{365} were 0.71 ± 0.16 m^2 g^{-1}, 0.51 ± 0.12 m^2 g^{-1}, 0.27 ± 0.06 m^2 g^{-1}, and 0.58 ± 0.05 m^2 g^{-1} for winter, pre-monsoon, monsoon and post-monsoon, respectively (Table 1). MAC_{365} values in the water extracts are similar or higher than those in methanol extracts during winter, pre-monsoon, monsoon seasons, which indicates that water-insoluble carbon extracted by methanol does not have higher light-absorbing properties per mass compared to WSOC at short wavelength.

The highest MAC_{365} values during winter indicated that organic aerosol absorbs UV–visible light more efficiently in winter than other seasons. The MAC_{365} values of WS-BrC and MeS-BrC were similar during the winter and monsoon seasons. And larger differences of MAC_{365} values between WS-BrC and MeS-BrC were obtained during the pre-monsoon and post-monsoon. The lowest MAC_{365} values for WS-BrC and MeS-BrC can be attributed to the efficiently wet scavenging and chemical components during the monsoon season.

The high MAC_{365} values during winter are comparable with the MAC values measured previously at NCO-P Station in winter during 2013–2014 (0.61–0.71 m^2 g^{-1}) in PM_{10} (Kirillova et al., 2016), on the Indo-Gangetic Plain (0.78 ± 0.24 m^2 g^{-1}) in $PM_{2.5}$ (Srinivas and Sarin, 2014) and over the Bay of Bengal (0.6 ± 0.2 m^2 g^{-1}) in TSP in November 2008 (Srinivas and Sarin, 2013). By contrast, the lower monsoon values

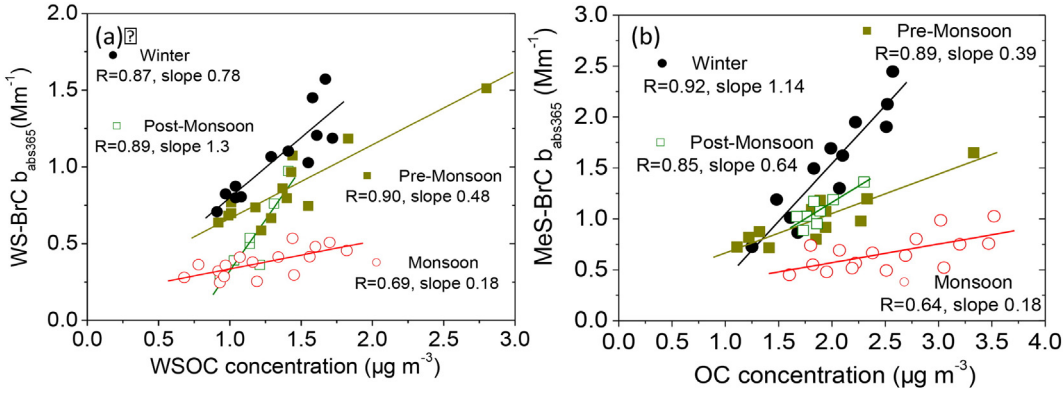

Fig. 4. Scatter plots for (a) WS-BrC b_{abs} at 365 nm and mass concentration of water-soluble organic carbon (WSOC), and (b) MeS-BrC b_{abs} at 365 nm and mass concentration of organic carbon (OC).

were obtained in the present study compared to the MAC_{365} data from low-altitude stations in remote areas of the Bay of Bengal and the Indian Ocean ($0.4 \pm 0.1\ m^2\ g^{-1}$) in PM_{10} in January 2009 (Srinivas and Sarin, 2013); $0.46 \pm 0.18\ m^2\ g^{-1}$ in $PM_{2.5}$ (Bosch et al., 2014). The values of WS-BrC and MeS-BrC MAC_{365} at Lulang are lower than those in the pollution source regions on the Indo-Gangetic Plain: the megacity New Delhi ($1.6 \pm 0.5\ m^2\ g^{-1}$) in $PM_{2.5}$ (Kirillova et al., 2014) and Patiala ($1.3 \pm 0.7\ m^2\ g^{-1}$) in $PM_{2.5}$ (Srinivas et al., 2016). These data show that the BrC tends to have higher MAC_{365} values in polluted conditions. However, the lowest MAC_{365} values of WS-BrC and MeS-BrC are reported during the monsoon season with the highest TC and OC concentrations in the present study.

MAC_{365} values in winter at Lulang are comparable with the WS-BrC MAC_{365} values measured in the East Asian outflow at Gosan site on Jeju Island ($0.65–0.75\ m^2\ g^{-1}$ in $PM_{2.5}$ and TSP) and in Beijing during summer ($0.51–0.73\ m^2\ g^{-1}$ in $PM_{2.5}$), but lower than in Beijing during winter time ($1.26–1.79\ m^2\ g^{-1}$ in $PM_{2.5}$) (Cheng et al., 2011; Du et al., 2014; Yan et al., 2015). In conclusion, the MAC_{365} determined at Lulang fall in the range of values observed in South and East Asia.

The large seasonal variations of MAC_{365} were observed, which indicated that MAC value was not governed solely by absorbing efficient, but also influenced by WSOC and OC levels, and as well as aerosol size distribution. For example, high MAC might also be partially caused by smaller mass median aerodynamic diameter of fine particles (Cheng et al., 2015).

3.2.3. Wavelength dependence of BrC light absorption

The summary of the calculated absorption Ångström Exponent (AAE) of BrC at Lulang was shown in Fig. 5. The wavelength dependence of the light absorption in the UV/visible range by WS-BrC and MeS-BrC did not exhibit a clear seasonal variability (Fig. 5, and Table 1). The seasonal average values of WS-BrC AAE within 365–550 nm range (6.7 ± 0.8 winter, 6.6 ± 0.6 pre-monsoon, 7.2 ± 0.9 monsoon, and 7.7 ± 1.3 post-monsoon) are higher than AAE values measured previously in Nepal Climate Observatory-Pyramid (4.9 ± 0.7 afternoon, 4.6 ± 0.8 night, 330–500 nm) (Kirillova et al., 2016), in New Delhi in winter (5.1 ± 2.0, 330–400 nm) (Kirillova et al., 2014), over the Indo-Gangetic Plain (IGP) in winter (6.0 ± 1.1, 300–700 nm) (Srinivas and Sarin, 2014). However, the AAE values in the present study are lower than AAE of the IGP outflow measured over the Bay of Bengal during winter months in 2008–2009 (9.1 ± 2.5, 300–700 nm) (Srinivas and Sarin, 2013).

The average values of MeS-BrC AAE within 365–550 nm (8.2 ± 1.4 winter, 8.4 ± 0.9 pre-monsoon, 8.1 ± 0.9 monsoon, and 8.0 ± 1.0 post-monsoon) are higher than those in methanol extracts from Nepal Climate Observatory-Pyramid (4.0 ± 1.0 afternoon, 3.7 ± 1.3 night, 330–500 nm) (Kirillova et al., 2016), from Los Angeles Basin (4.82 ± 0.49, 300–600 nm) (Zhang et al., 2013) and in an urban site of Atlanta, GA (4.98, 300–500 nm) (Liu et al., 2013). However, the comparison of AAE values from different studies is challenging as they are fitted within different wavelength ranges. AAE of MeS-BrC was on average slightly higher than that of WS-BrC within 365–550 nm wavelength range (Fig. 5). The changes observed in AAEs can be attributed to the variations in the chemical composition or in the particle size (Sandradewi et al., 2008).

4. Conclusions and implications

The light absorbing properties of the WS-BrC and MeS-BrC were investigated at Lulang in the southeastern margin of the Tibetan Plateau. The light absorption coefficients of WS-BrC and MeS-BrC followed the seasonal trends of WSOC and OC, respectively. The highest levels of TC ($3.3 \pm 0.7\ \mu g\ m^{-3}$) and OC ($2.5 \pm 0.6\ \mu g\ m^{-3}$) were observed in the monsoon season. Winter b_{abs365} ($1.04\ Mm^{-1}$ for WS-BrC and $1.47\ Mm^{-1}$ for MeS-BrC) were much higher than those for monsoon (WS-BrC for $0.38\ Mm^{-1}$ and MeS-BrC for $0.67\ Mm^{-1}$). MeS-BrC absorbs about 1.5 times higher at 365 nm compared to WS-BrC. The positive relationship between WSOC (OC) and WS-BrC (MeS-BrC) b_{abs365} illustrated that BrC was the dominant absorption material in extracts and having similar sources to WSOC and OC. The values of AAE (365–550 nm) were lower for WS-BrC (6.9) compared to MeS-BrC (8.2). The MAC_{365} values varied from 0.3 (monsoon) to 0.8 (winter) for both of MeS-BrC and WS-BrC. The observed BrC MAC_{365} was within the range of the results measured previously at the low-altitude sites and indicating higher potential effects on climate at the high-altitude area. The highest MAC_{365} values in winter indicated the BrC with further

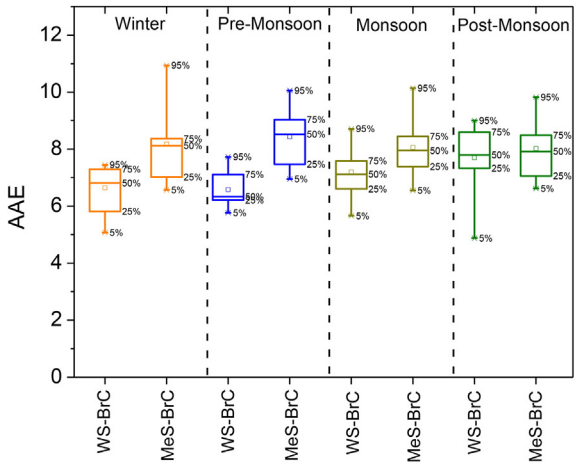

Fig. 5. The variations of BrC Ångström Exponent (AAE) calculated within the wavelength ranges 365–550 nm for water and methanol extracts of the TSP samples.

oxidation and ages may become more absorbing. Considering the potential effects on climate and the impact on glaciers in TP, the sources, synoptic changes of BrC should receive special attention in future research.

Acknowledgements

This research was funded by the National Natural Science Foundation of China (41771518, 41230641, and 41673134). The authors are grateful to the South-East Tibetan plateau Station for integrated observation and research of alpine environment for the assistance with filed sampling.

References

Alexander, D.T.L., Crozier, P.A., Anderson, J.R., 2008. Brown carbon spheres in East Asian outflow and their optical properties. Science 321, 833–836.

Andreae, M.O., Gelencsér, A., 2006. Black carbon or brown carbon? The nature of light-absorbing carbonaceous aerosol. Atmos. Chem. Phys. 6, 3131–3148.

Bosch, C., Andersson, A., Kirillova, E.N., Budhavant, K., Tiwari, S., Praveen, P.S., Russell, L.M., Beres, N.D., Ramanathan, V., Gustafsson, Ö., 2014. Source-diagnostic dual-isotope composition and optical properties of water-soluble organic carbon and elemental carbon in the South Asian outflow intercepted over the Indian Ocean. J. Geophys. Res. 119:11,743–11,759. https://doi.org/10.1002/2014JD022127.

Cao, J.J., Lee, S.C., Ho, K.F., Zhang, X.Y., Zou, S.C., Fung, K.K., Chow, J.C., Watson, J.G., 2003. Characteristics of carbonaceous aerosol in Pear River Delta Region, China during 2001 winter period. Atmos. Environ. 37, 1451–1460.

Cao, J.J., Xu, B.Q., He, J.Q., Liu, X.Q., Han, Y.M., Wang, G.H., Zhu, C.S., 2009. Concentration, seasonal variations, and transport of carbonaceous aerosols at a remote mountainous region in western China. Atmos. Environ. 43, 4444–4452.

Cao, J.J., Tie, X.X., Xu, B.Q., Zhao, Z.Z., Zhu, C.S., Li, G.H., Liu, S.X., 2010. Measuring and modeling black carbon (BC) contamination in the SE Tibetan Plateau. J. Aerosol Sci. 67, 45–60.

Chen, Y., Bond, T.C., 2010. Light absorption by organic carbon from wood combustion. Atmos. Chem. Phys. 10, 1773–1787.

Cheng, Y., He, K.B., Zheng, M., Duan, F.K., 2011. Mass absorption efficiency of elemental carbon and water-soluble organic carbon in Beijing, China. Atmos. Chem. Phys. 11, 497–11,510.

Cheng, C.L., Wang, G.H., Meng, J.J., Wang, Q.Y., Cao, J.J., Li, J.J., Wang, J.Y., 2015. Size-resolved airborne particulate oxalic and related secondary organic aerosol species in the urban atmosphere of Chengdu, China. Atmos. Res. 161–162, 134–142.

Chow, J.C., Watson, J.G., Chen, L.W.A., Chang, M.C.O., Robinson, N.F., Trimble, D., Kohl, S., 2007. The IMPROVE-A temperature protocol for thermal/optical carbon analysis: maintaining consistency with a long-term database. J. Air Waste Manage. Assoc. 57, 1014–1023.

Chow, J.C., Watson, J.G., Robles, J., Wang, X., Chen, L.W., Trimble, D.L., Kohl, S.D., Tropp, R.J., Fung, K.K., 2011. Quality assurance and quality control for thermal/optical analysis of aerosol samples for organic and elemental carbon. Anal. Bioanal. Chem. 401, 3141–3152.

Cong, Z., Kang, S., Gao, S., Zhang, Y., Li, Q., Kawamura, K., 2013. Historical trends of atmospheric black carbon on Tibetan Plateau as reconstructed from a 150-year lake sediment record. Environ. Sci. Technol. 47, 2579–2586.

Du, Z., He, K., Cheng, Y., Duan, F., Ma, Y., Liu, J., Zhang, X., Zhang, M., Weber, R., 2014. A year long study of water-soluble organic carbon in Beijing II: light absorption properties. Atmos. Environ. 89, 235–241.

Ganguly, D., Jayaraman, A., Rajesh, T.A., Gadhavi, H., 2006. Wintertime aerosol properties during foggy and nonfoggy days over urban center Delhi and their implications for shortwave radiative forcing. J. Geophys. Res. 111, D15217. https://doi.org/10.1029/2005JD007029.

Hecobian, A., Zhang, X., Zheng, M., Frank, N., Edgerton, E.S., Weber, R.J., 2010. Water-soluble organic aerosol material and the light-absorption characteristics of aqueous extracts measured over the Southeastern United States. Atmos. Chem. Phys. 10, 5965–5977.

Kirillova, E.N., Andersson, A., Tiwari, S., Srivastava, A.K., Bisht, D.S., Gustafsson, Ö., 2014. Water-soluble organic carbon aerosols during a full New Delhi winter: isotope-based source apportionment and optical properties. J. Geophys. Res. 119: 3476–3485. https://doi.org/10.1002/2013JD020041.

Kirillova, E.N., Marinoni, A., Bonasoni, P., Vuillermoz, E., Facchini, M.C., Fuzzi, S., Decesari, S., 2016. Light absorption properties of brown carbon in the high Himalayas. J. Geophys. Res. 121:9621–9639. https://doi.org/10.1002/2016JD025030.

Lack, D.A., Langridge, J.M., 2013. On the attribution of black and brown carbon light absorption using the Ångström exponent. Atmos. Chem. Phys. 13, 10,535–10,543.

Laskin, A., Laskin, J., Nizkorodov, S.A., 2015. Chemistry of atmospheric brown carbon. Chem. Rev. 115, 4335–4382.

Liu, J., Bergin, M., Guo, H., King, L., Kotra, N., Edgerton, E., Weber, R.J., 2013. Size-resolved measurements of brown carbon in water and methanol extracts and estimates of their contribution to ambient fine-particle light absorption. Atmos. Chem. Phys. 13: 12,389–12,404. https://doi.org/10.5194/acp-13-12389-2013.

Marinoni, A., Cristofanelli, P., Laj, P., Duchi, R., Calzolari, F., Decesari, S., Sellegri, K., Vuillermoz, E., Verza, G.P., Villani, P., Bonasoni, P., 2010. Aerosol mass and black carbon concentrations, a two year record at NCO-P (5079 m, Southern Himalayas). Atmos. Chem. Phys. 10, 8551–8562.

Moosmüller, H., Chakrabarty, R.K., Ehlers, K.M., Arnott, W.P., 2011. Absorption Ångström coefficient, brown carbon, and aerosols: basic concepts, bulk matter, and spherical particles. Atmos. Chem. Phys. 11, 1217–1225.

Mouli, P., Mohan, S., Reddy, S., 2006. Chemical composition of atmospheric aerosol (PM10) at a semi-arid urban site: influence of terrestrial sources. Environ. Monit. Assess. 117 (1), 291–305.

Pöschl, U., 2003. Aerosol particle analysis: challenges and progress. Anal. Bioanal. Chem. 375, 30–32.

Ramanathan, V., Ramana, M.V., Roberts, G., Kim, D., Corrigan, C.E., Chung, C.E., Winker, D., 2007a. Warming trends in Asia amplified by brown cloud solar absorption. Nature 448, 575–578.

Ramanathan, V., Li, F., Ramana, M.V., Praveen, P.S., Kim, D., Corrigan, C.E., Nguyen, H., Stone, E.A., Schauer, J.J., Carmichae, G.R., Adhikary, B., Yoon, S.C., 2007b. Atmospheric brown clouds: Hemispherical and regional variations in long-range transport, absorption, and radiative forcing. J. Geophys. Res. 112, D22S21. https://doi.org/10.1029/2006JD008124.

Sandradewi, J., Prevot, A.S.H., Szidat, S., Perron, N., Alfarra, M.R., Lanz, V.A., Weingartner, E., Baltensperger, U., 2008. Using aerosol light absorption measurements for the quantitative determination of wood burning and traffic emission contributions to particulate matter. Environ. Sci. Technol. 42, 3316–3323.

Shen, Z.X., Cao, J.J., Zhang, L.M., Liu, L., Zhang, Q., Li, J., Han, Y.M., Zhu, C.S., Zhao, Z.Z., Liu, S. X., 2014. Day–night differences and seasonal variations of chemical species in PM_{10} over Xi'an, northwest China. Environ. Sci. Pollut. Res. 21, 3697–3705.

Shrestha, A.B., Wake, C.P., Dibb, J.E., Mayewski, P.A., Whitlow, S.I., Carmichael, G.R., Ferm, M., 2000. Seasonal variations in aerosol concentrations and compositions in the Nepal Himalaya. Atmos. Environ. 34, 3349–3363.

Srinivas, B., Sarin, M.M., 2013. Light-absorbing organic aerosols (brown carbon) over the tropical Indian Ocean: impact of biomass burning emissions. Environ. Res. Lett. 8, 7. https://doi.org/10.1088/1748-9326/8/4/044042.

Srinivas, B., Sarin, M.M., 2014. Brown carbon in atmospheric outflow from the Indo-Gangetic Plain: mass absorption efficiency and temporal variability. Atmos. Environ. 89, 835–843.

Srinivas, B., Rastogi, N., Sarin, M.M., Singh, A., Singh, D., 2016. Mass absorption efficiency of light absorbing organic aerosols from source region of paddy-residue burning emissions in the Indo-Gangetic Plain. Atmos. Environ. 125, 360–370.

Sun, H.L., Biedermann, L., Bond, T.C., 2007. Color of brown carbon: a model for ultraviolet and visible light absorption by organic carbon aerosol. Geophys. Res. Lett. 34, L17813. https://doi.org/10.1029/2007GL029797.

Wang, G.H., Xie, M., Hu, S., Gao, S., Tachibana, E., Kawamura, K., 2010. Dicarboxylic acids, metals and isotopic compositions of C and N in atmospheric aerosols from inland China: implications for dust and coal burning emission and secondary aerosol formation. Atmos. Chem. Phys. 10:6087–6096. https://doi.org/10.5194/acp-10-6087-2010.

Wang, M., Xu, B.Q., Zhao, H.B., Cao, J.J., Joswiak, D., Wu, G., Lin, S., 2012. The influence of dust on quantitative measurements of black carbon in ice and snow when using a thermal optical method. Aerosol Sci. Technol. 46 (1), 60–69.

Wang, G.H., Zhou, B.H., Cheng, C.L., Cao, J.J., Li, J.J., Meng, J.J., Tao, J., Zhang, R.J., Fu, P.Q., 2013. Impact of Gobi desert dust on aerosol chemistry of Xi'an, inland China during spring 2009: differences in composition and size distribution between the urban ground surface and the mountain atmosphere. Atmos. Chem. Phys. 13:819–835. https://doi.org/10.5194/acp-13-819-2013.

Xu, B.Q., Cao, J.J., Hansen, J., Yao, T.D., Joswia, D.R., Wang, N.L., Wu, G.J., Wang, M., Zhao, H. B., Yang, W., Liu, X.Q., He, J.Q., 2009. Black soot and the survival of Tibetan glaciers. Proc. Natl. Acad. Sci. 106 (52), 22114–22118.

Xu, B.Q., Cao, J.J., Joswiak, D.R., Liu, X.Q., Zhao, H.B., He, J.Q., 2012. Post-depositional enrichment of black soot in snow-pack and accelerated melting of Tibetan glaciers. Environ. Res. Lett. 7 (1), 17–35.

Yan, C.Q., Zheng, M., Sullivan, A.P., Bosch, C., Desyaterik, Y., Andersson, A., Li, X.Y., Guo, X. S., Zhou, T., Gustafsson, O., Collett Jr., Jeffrey L., 2015. Chemical characteristics and light-absorbing property of water-soluble organic carbon in Beijing: biomass burning contributions. Atmos. Environ. 121, 4–12.

Yao, T.D., Thompson, L.G., Mosbrugger, V., Zhang, F., Ma, Y.M., Luo, T.X., Xu, B.Q., Yang, X. X., Joswiak, D.R., Wang, W.C., Joswiak, M.E., Devkota, L.P., Tayal, S., Jilani, R., Fayziev, R., 2012. The third pole environment (TPE). Environ. Dev. 3, 52–64.

Zhang, X.L., Lin, Y.H., Surratt, J.D., Zotter, P., Prevot, A.S., Webber, R.J., 2011. Light-absorbing soluble organic aerosol in Los Angeles and Atlanta: a contrast in secondary organic aerosol. Geophys. Res. Lett. 38, L21810.

Zhang, X.L., Lin, Y.H., Surratt, J.D., Weber, R.J., 2013. Sources, composition and absorption Ångström exponent of light-absorbing organic components in aerosol extracts from the Los Angeles Basin. Environ. Sci. Technol. 47, 3685–3693.

Zhao, Z.Z., Cao, J.J., Shen, Z.X., Xu, B.Q., Zhu, C.S., Antony Chen, L.W., Su, X.L., Liu, S.X., Han, Y.M., Wang, G.H., Ho, K.F., 2013. Aerosol particles at a high altitude site on the Southeast Tibetan Plateau, China: implications for pollution transport from South Asia. J. Geophys. Res. 118 (19), 11360–11375.

Zhu, C.S., Cao, J.J., Hu, T.F., Shen, Z.X., Tie, X.X., Huang, H., Wang, Q.Y., Huang, R.J., Zhao, Z.Z., Močnik, G., Hansen, A.D.A., 2017. Spectral dependence of aerosol light absorption at an urban and a remote site over the Tibetan Plateau. Sci. Total Environ. 590–591, 14–21.